Available online at www.sciencedirect.com
ScienceDirect
Cement and Concrete Research 36 (2006) 1425–1433
Cement and Concrete Research

Influence of compaction on the interfacial transition zone and the permeability of concrete

Andreas Leemann *, Beat Münch, Philippe Gasser, Lorenz Holzer

EMPA, Swiss Federal Institute for Materials Testing and Research, Überlandstr. 129, 8600 Dübendorf, Switzerland

Received 15 August 2005; accepted 10 February 2006

Abstract

The interfacial transition zone (ITZ) is regarded as a key feature for the transport properties and the durability of concrete. In this study one self-compacting concrete (SCC) mixture and two conventionally vibrated concrete (CVC) mixtures are studied in order to determine the influence of compaction on the porosity of the ITZ. Additionally oxygen permeability and water conductivity were measured in vertical and horizontal direction. The quantitative analysis of images made with an optical microscope and an environmental scanning electron microscope shows a significantly increased porosity and width of the ITZ in CVC compared to SCC. At the same time oxygen permeability and water conductivity of CVC are increased in comparison to SCC. Moreover, considerable differences in the porosity of the lower, lateral and upper ITZ are observed in both types of concrete. The anisotropic distribution of pores in the ITZ does not necessarily cause anisotropy in oxygen permeability and water conductivity though.

Keywords: Vibration; Interfacial transition zone; Porosity; Permeability; Self-compacting concrete

1. Introduction

The porosity in the interfacial transition zone (ITZ) of mortar and concrete is increased compared to the bulk of the hardened paste [1,2]. This is mainly attributed to the "wall effect" leading to a relatively low concentration of large cement particles in the ITZ and consequently to an increased porosity [3]. During cement hydration the pores in the ITZ get partly filled mainly due to a redistribution of calcium hydroxide and C–S–H [4]. The ITZs of individual aggregates can be interconnected depending on their width and the content of aggregates. Such connectivity or percolation is regarded by many authors as a key feature governing the permeability and transport properties of mortar and concrete [e.g. 5,6]. But the concept of percolation is not universally accepted due to the inhomogeneous distribution of porosity in the ITZ and the bulk paste [7].

There are several factors influencing the properties of the ITZ. Its width increases with increasing water/binder-ratio (w/b) and aggregate/cement-ratio [8]. The composition and particle size distribution of the binder can affect the porosity of the ITZ; the addition of microsilica has been shown to decrease its porosity [9]. When the mixing time of a concrete is short the ITZ is less pronounced compared to a well mixed concrete [7]. The type of compaction may have an influence; qualitative observations have shown that the increase of porosity in the ITZ of self-compacting concrete (SCC) seems to be less pronounced compared to conventionally vibrated concrete (CVC) [10]. Additionally segregation, bleeding and settlement may have an influence on the porosity of the ITZ. Because the latter processes are influenced by gravity they may lead to an anisotropic ITZ with increased porosity at the bottom of aggregates and decreased porosity at the top [11]. Consequently, this anisotropy may cause differences in the transport properties of the concrete in either horizontal or vertical direction [12].

So far the focus of research in SCC has been mainly on mix design and mechanical properties [13,14]. Relatively little work has been done on the durability and microstructure of SCC in spite of its increasing use worldwide. In order to obtain a better understanding about the differences between SCC and CVC the influence of compaction on the porosity of the ITZ needs to be investigated. In this study, the interfacial microstructure of a SCC and two CVC is characterized using an optical microscope (OM) and an environmental scanning electron microscope

* Corresponding author. Tel.: +41 44 823 44 89; fax: +41 44 823 40 35.
E-mail address: andreas.leemann@empa.ch (A. Leemann).

0008-8846/$ - see front matter © 2006 Elsevier Ltd. All rights reserved.
doi:10.1016/j.cemconres.2006.02.010

Table 1
Composition and workability of the concrete

	SCC	CVC 1	CVC 2
Aggregate [kg/m^3]	1700	1700	1920
Grain size [mm]	0–16	0–16	0–32
Sand/gravel ratio	1.0	1.0	0.54
Cement [kg/m^3]	465	465	360
Superplasticizer [kg/m^3]	7.9	1.9	1.4
Water [kg/m^3]	181	181	140
Volume of paste [l/m^3]	330	330	255
W/b-ratio	0.39	0.39	0.39
Slump flow [cm]	64	–	–
Flow time L-box [s]	2.8	–	–
Flow [cm]	–	58	35

(ESEM). The volume and distribution of pores was quantified by image analysis software. Furthermore, the influence of the porosity of the ITZ and its possible anisotropy on oxygen permeability and water conductivity were examined.

2. Methods and materials

The composition of the SCC and CVC 1 was identical apart from the dosage of superplasticizer (SP) (Table 1). Therefore, it should be possible to attribute any differences in microstructure and transport properties between these two mixes to compaction. The w/b of CVC 2 was identical with the SCC and CVC 1. But the volume of paste and sand was reduced and the maximum grain size was increased. Any differences of CVC 2 compared to CVC 1 should be attributed to the variation of these parameters. Regarding the volume of paste and the grain size distribution CVC 2 represents a typical CVC used in Switzerland.

Ordinary Portland cement CEM I 42.5 (Blaine: 2980 cm^2/g, density: 3.13 kg/m^3) was used for the SCC and the two CVCs (Table 2). The mixes were produced with natural sand and gravel as aggregate. The SP used is based on polycarboxylate ether. A pan-type mixer was used to produce the concrete. The mixing time of the components was 120 s. The workability of the SCC was determined using an Abraham's cone and an L-box [15]. The slump of the CVC was measured according to Ref. [16]. Assessed visually, all three mixes were stable and did not exhibit signs of segregation. Two small prisms ($l \times d \times h = 36 \times 12 \times 12$ cm^3) and one large prism ($l \times d \times h = 60 \times 30 \times 30$ cm^3) were produced from each mix. CVC 1 and CVC 2 were compacted with a vibrator (Dynapac AH15) immediately after casting. The vibrator has a front element with a length of 330 mm and a diameter of 40 mm. It vibrates with a frequency of 270 Hz and an amplitude of 0.40 mm. The concrete was vibrated until its upper surface was smooth and no signs of further compaction like rising air bubbles were observed. The prisms were cast and stored in a room at 20 °C and 90% relative humidity.

Table 2
Composition of the CEM I 42.5

CaO [%]	SiO_2 [%]	Al_2O_3 [%]	Fe_2O_3 [%]	MgO [%]	K_2O [%]	Na_2O [%]	SO_3 [%]	Loss on ignition [%]
63.5	19.8	4.6	2.5	1.8	0.89	0.10	3.2	2.7

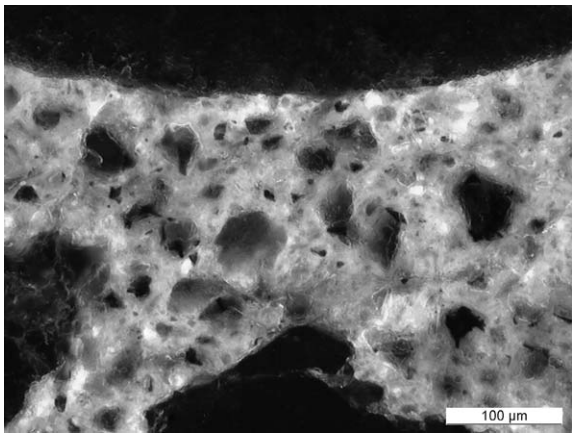

Fig. 1. Paste below an aggregate (OM).

The examination of the concrete was conducted at an age of 28 days. Compressive strength was determined on the prisms ($12 \times 12 \times 36$ cm) stored at 20 °C and 90% relative humidity according to Ref. [17]. Cores with a diameter of 50 and 68 mm were taken from the large prisms in vertical and horizontal directions. Water conductivity according to Ref. [17] was determined on 30 cores (diameter and height of 50 mm) per prism. The values were calculated based on water sorption of the preconditioned samples, their total water take up and their overall porosity. The oxygen permeability (OP) coefficient was measured on cores with a diameter of 68 mm and a height of 25 mm following the method presented in Ref. [18]. The test method is based on the decrease of the applied pressure gradient due to oxygen passing through the samples. 22 cores were measured per prism.

From each mix the uppermost 12 cm from a vertical core with a diameter of 50 mm were used to prepare the samples for the microscopic investigation. The cores were sawn in two halves and dried for three days at 50 °C. They were impregnated with an epoxy resin containing a fluorescent dye. One half was used to prepare thin sections (area of 50×60 mm^2) with a

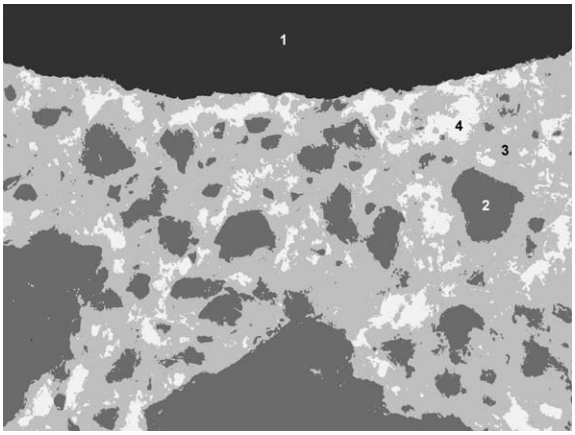

Fig. 2. Identified classes. Black: aggregate (1), dark grey: aggregates and anhydrous cement (2), grey: unspecified areas (3), and light grey: porous paste (4).

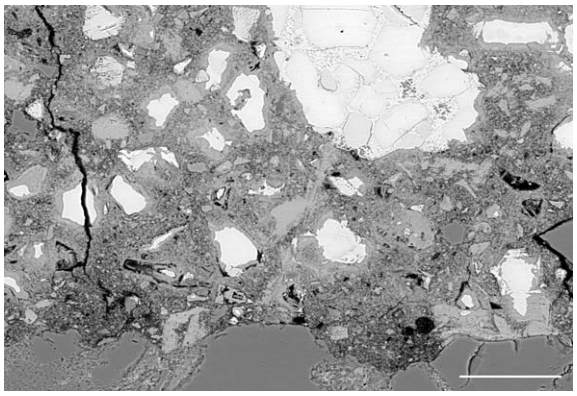

Fig. 3. Paste above an aggregate (ESEM). White bar measures 50 μm.

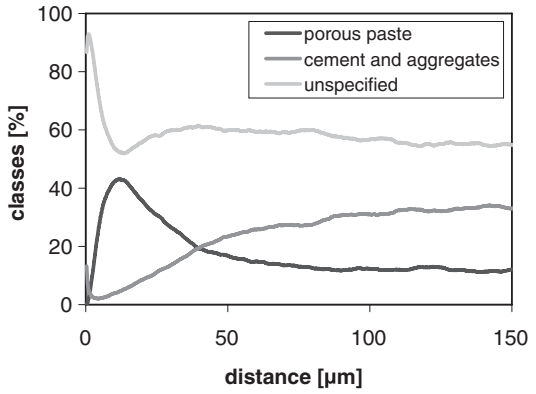

Fig. 5. Distribution of porous paste and cement/aggregates in the lower ITZ of the SCC (OM).

thickness of 30 μm. The other half was used to produce polished samples (area of 50×60 mm^2) for the ESEM.

The thin sections were studied with a Zeiss Axioplan. The incident-light illumination of the OM excites the fluorescent dye in the epoxy resin in the whole thickness of the thin section. Therefore, luminescence of the images is proportional to the porosity and represents an average for the thickness of the thin section. As a result, the transitions of the different components of the concrete like aggregates and hardened paste are gradual. A lot of pores in the concrete have a diameter smaller than 30 μm. They cannot be identified individually due to the thickness of the thin section. But they increase the luminosity of the paste. The appearance of the transition zone between aggregate and paste is influenced by two factors. Firstly, aggregates are not opaque and some of the fluorescence of the paste illuminates the edge of the aggregates. This translucency is dependent on the type of aggregate. Secondly, the edge of an aggregate is sharp and its transition to the paste is well defined only when the tangent of its surface is parallel to the optical axis of the microscope lens. When the aggregate is not cut equatorially and the tangent of its surface is not parallel to the microscope lens, the transition is poorly defined with a gradual change from the dark aggregate to the bright paste usually measuring 5–20 μm. In the first case, the distances measured in two dimensional sections represent the true perpendicular distance to the aggregate in three dimensions. An overestimation of the distance to the aggregate results when a section does not cut an aggregate perpendicular to its surface. For the investigation with the OM aggregates with sharp edges were chosen in order to minimise an overestimation of ITZ thickness due to effects of sectioning. Therefore, no factor was used to correct the distances measured between the analysed classes. After marking all aggregates with sharp edges 35 of them were randomly selected for each concrete mix. Digital images of these aggregates were made with a Sony DKC-5000 mounted on the Zeiss Axioplan. The illumination intensity was identical for all images. The images have a resolution of 1520×1144 pixels (pixel size: 0.33×0.33 μm). Six images were made for each aggregate studied; two at the top, two at the side (alternately on the right or the left side) and two at the base of each aggregate resulting in 192 images per concrete.

The polished samples for the ESEM were examined with the OM first. The aggregates were selected in the same manner as the aggregates studied in the thin sections. They were studied with a Phillips ESEM-FEG XL30. The samples were not coated and the operating conditions of the ESEM were 15 kV and 1.0 Torr in the low vacuum mode using a back scatter detector. 25 aggregates were studied per concrete mix. The images taken have a resolution of 1420×968 pixels (pixel size: 0.22×0.24 μm). Nine images were made per aggregate studied;

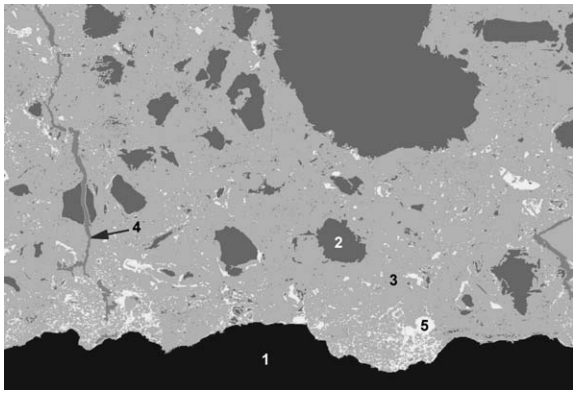

Fig. 4. Identified classes. Black: aggregate (1), dark grey: anhydrous cement (2), grey: background (3), light grey: unspecified areas (paste and aggregates/4), and white: pores (5).

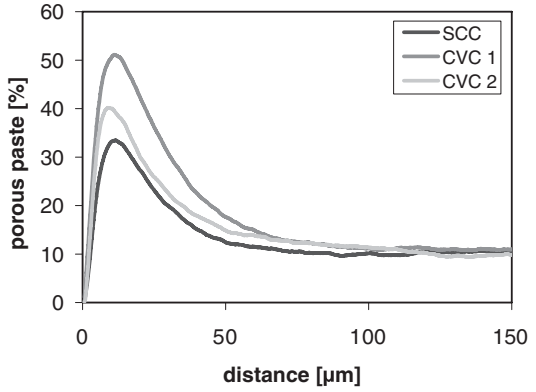

Fig. 6. Average volume of porous paste in the ITZ (OM). Number of images analysed per concrete: 192.

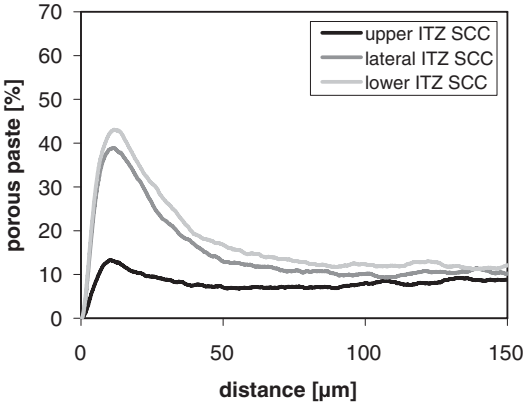

Fig. 7. Volume distribution of porous paste in the ITZ of the SCC (OM).

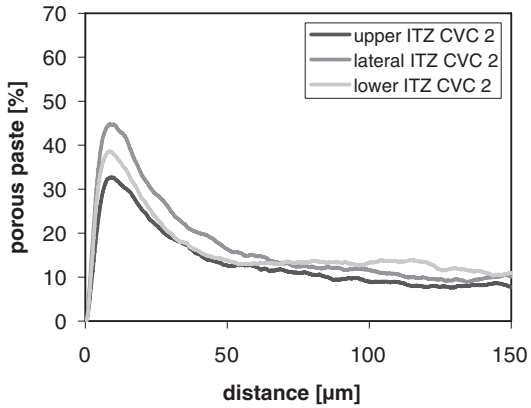

Fig. 9. Volume distribution of porous paste in the ITZ of CVC 2 (OM).

three at the top, three at the side (alternately on the right or the left side) and three at the base of each aggregate resulting in 225 images per concrete.

The software for image analysis has been developed in a Matlab 6.5 environment. It supports a fast interactive segmentation. For the segmentation of OM images four different classes were defined based on their grey level values; main aggregate, residual aggregates and anhydrous cement, porous paste and background (Figs. 1 and 2). Cracks and large air voids were defined as "background". The threshold value to identify porous paste was kept constant for all samples in order to obtain comparable results while the threshold to identify aggregates and cement grains was adjusted individually for each image to optimize the fit. The latter step was necessary to compensate for the varying translucency of the aggregates that was mainly caused by variations in the luminescence of the surrounding paste. The threshold was chosen in a way that a minimal amount of porous paste was detectable even in the densest parts of the thin sections. Four different classes were made in the ESEM images; main aggregate, pores, cement grains and background. Again cracks and large air voids were defined as "background" (Figs. 3 and 4).

The relative volume share of each different class in the OM and ESEM images was analysed as a function of its distance to the aggregate. The calculation accuracy was one pixel.

The ITZ was defined as the area where the volume of porous paste (OM) and pores (ESEM) were 20% higher than in the bulk paste.

3. Results

3.1. OM

The distribution of porosity is very inhomogeneous throughout the paste of all three mixes. Areas of porous paste are distributed in a patchy manner along the interface and in the bulk paste (Figs. 1 and 2). The occurrence of such patches seems to increase with decreasing distance from the aggregates.

The quantitative analysis verifies the qualitative observation. In all three mixes the volume of porous paste increases and the volume of aggregates and anhydrous cement decreases on a profile towards the interface (Fig. 5). The width of the ITZ in the three mixes varies. The zone of increased porosity (average values for upper lateral and lower ITZ) is about 70 µm wide in CVC 1 and CVC 2 and about 50 µm in the SCC (Fig. 6). The maximum volume of porous paste occurs at a distance of about 10 µm from the aggregates in all three mixes. After reaching this maximum there is a sharp drop towards the aggregates. This is a particularity of the method used. The predominate part of the area in this 10 µm thick shell between maximum porosity and

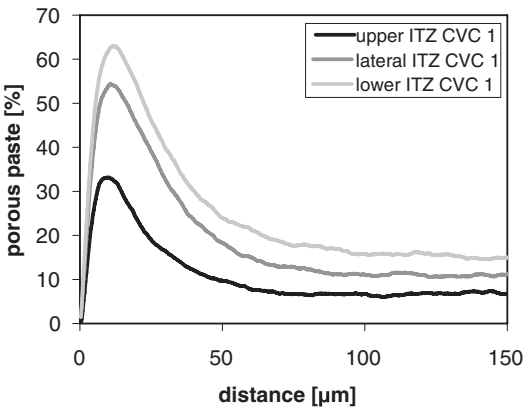

Fig. 8. Volume distribution of porous paste in the ITZ of CVC 1 (OM).

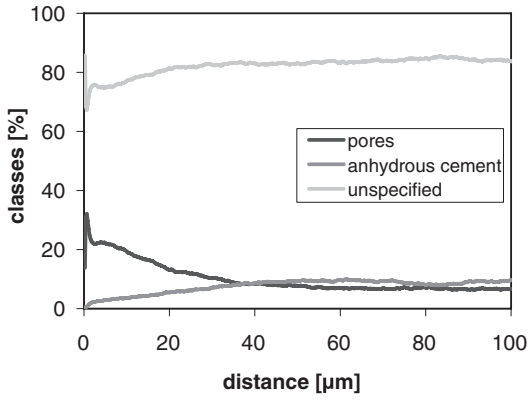

Fig. 10. Distribution of pores and anhydrous cement in the lower ITZ of the SCC (ESEM).

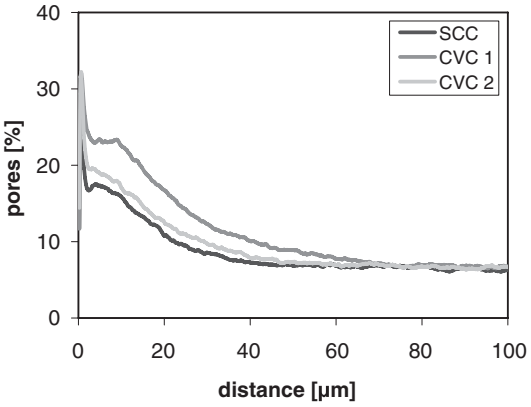

Fig. 11. Average volume of pores in the ITZ (ESEM). Number of images analysed per concrete: 225.

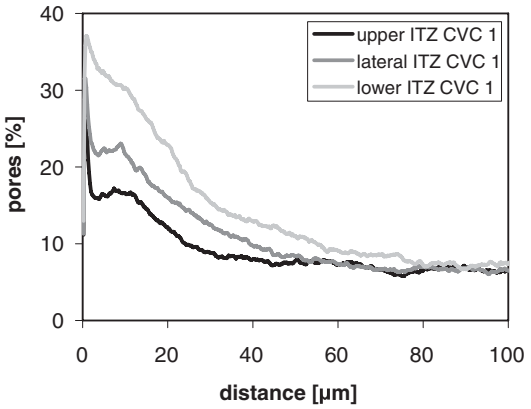

Fig. 13. Volume distribution of pores in the ITZ of CVC 1 (ESEM).

aggregate is classified as "unspecified" due to its grey value. This is an effect of the gradual transition between the different components caused by the thickness of the thin section and the partial translucency of the aggregates. Because the edge of the aggregates might be classified as "unspecified" due to their translucency the ITZ appears to be somewhat wider than in reality.

CVC 1 shows the highest value and the SCC the lowest. There are differences between the relative volume of porous paste below, at the side and above the aggregates (Figs. 7–9). The SCC and CVC 1 have a significantly lower porosity in the upper than in the lateral and lower ITZ. The porosity of the SCC is hardly increased above the aggregates. The porosity in the lateral ITZ is slightly lower than in the lower ITZ in the SCC and CVC 1. The relative differences are less pronounced in CVC 2.

About 50% of the cross-sections of the aggregates studied have diameters smaller than 4 mm. In general the ITZ of the small aggregates is slightly less porous than the one of the large aggregates in all three mixes.

Ten of the aggregates studied were located in the uppermost 2.5 cm of the prisms investigated. A comparison of the ITZ around these aggregates with the ones in greater depth shows no systematic difference in the three mixes. The qualitative difference in the microstructure observed in the thin sections is the occurrence of microcracks perpendicular to the surface of the concrete. The width of these microcracks is typically around 5 µm and they reach a depth between 5 and 15 mm. They are presumably caused by drying shrinkage.

3.2. ESEM

In the ESEM images the same patchy pattern of pore distribution already observed with the OM is present. Usually the diameter of such porous patches is below 0.5 mm. In the ITZ there are some patches elongated parallel to the aggregates. There seems to be an increase in the frequency of porous patches approaching the aggregates. Assessed qualitatively the pore diameter in the ITZ below the aggregates is larger in CVC 1 than in the SCC and CVC 2.

The quantitative analysis shows an increase in the volume of pores and a corresponding decrease in the volume of cement as the aggregates are approached (Fig. 10). The zone of increased porosity (average values for upper, lateral and lower ITZ) is about 40 µm wide in the SCC and CVC 2 and about 60 µm wide in CVC 1 (Fig. 11). After showing a decrease of the gradient in the region of about 10 µm to the analysed aggregates there is a sharp increase in the volume of pores about 3 µm away from the aggregates. The reason for this increase in the volume of pores

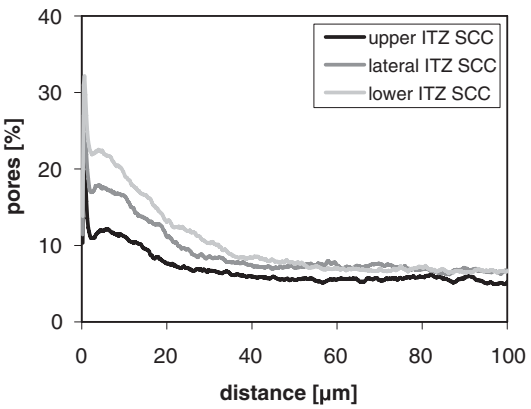

Fig. 12. Volume distribution of pores in the ITZ of the SCC (ESEM).

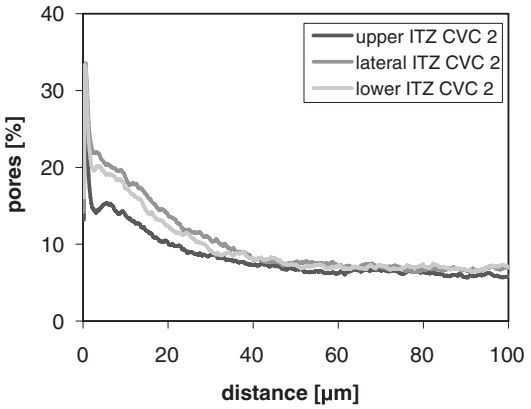

Fig. 14. Volume distribution of pores in the ITZ of CVC 2 (ESEM).

Table 3
Properties of the concrete

	SCC	CVC 1	CVC 2
Compressive strength [MPa]	69.5	63.4	70.8
Coefficient of variation [%]	2.5	1.9	2.5
OPC horizontally [10^{-11} m/s]	1.91	2.38	1.30
Coefficient of variation [%]	26.5	19.9	19.2
Bulk density [kg/m^3]	2325	2332	2421
OPC vertically [10^{-11} m/s]	1.90*	2.66*	2.11*
Coefficient of variation [%]	14.6*	38.2*	25.6*
Bulk density [kg/m^3]	2297	2321	2376
Water conductivity horizontally [g/m^2 h]	5.35	6.89	3.50
Coefficient of variation [%]	13.62	14.44	19.00
Bulk density [kg/m^3]	2312	2285	2392
Water conductivity vertically [g/m^2 h]	5.50	5.45	4.17
Coefficient of variation [%]	14.05	8.16	18.66
Bulk density [kg/m^3]	2293	2298	2390

*Covercrete excluded.

is not obvious. Recognizable bonding cracks were defined as background and do therefore not appear in the analysis of the pores. But the peak may be the result of bonding cracks that have a width in the range of the resolution of the images. Sometimes these cracks may be wide enough to be resolved and are classified as "pores" and sometimes they may be too narrow to be resolved and are classified as "unspecified". The cracks are most likely caused by the drying of the concrete before impregnation. However, the decrease of the gradient of the pore volume observed by ESEM at a distance to the aggregates of 10 μm is related to the deposition of calcium hydroxide at the edge of the aggregates. These deposits are dense and locally decrease the volume of pores.

In general, the volume of pores in the ITZ of CVC 1 is higher compared to the SCC and CVC 2. The relative volume of pores in the lower, lateral and upper ITZ differs (Figs. 12–14). In all three mixes the upper ITZ displays the lowest porosity. While the SCC and CVC 1 show a higher volume of pores in the lower than in the lateral ITZ the opposite applies to CVC 2. The same peculiarity appears in the analysis of the images made with the OM where the lateral ITZ of CVC 2 displays the highest porosity.

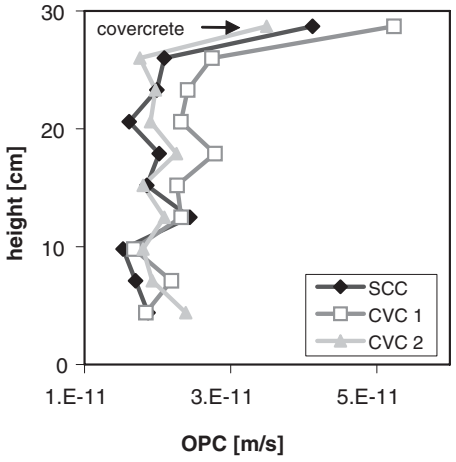

Fig. 15. Vertical distribution of OPC in the concrete prisms.

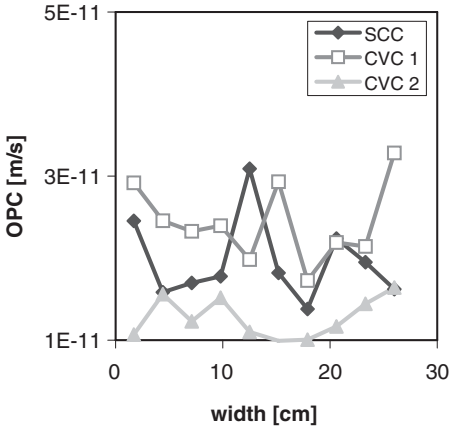

Fig. 16. Horizontal distribution of OPC in the concrete prisms.

The aggregates with a diameter of the cross-section below 4 mm have a slightly less porous ITZ than the larger aggregates but the zone of increased porosity has the same width.

Ten of the aggregates studied were located in the uppermost 2.5 cm of the prisms investigated. A comparison of the porosity of the ITZ shows that the aggregates in the uppermost 2.5 cm have a slightly higher porosity in the ITZ and in the bulk paste than the ones in greater depth. This applies to all three mixes.

3.3. Concrete properties

The SCC and CVC 2 exhibit about the same compressive strength and oxygen permeability (Table 3, Figs. 15 and 16). The compressive strength of CVC 1 is lower and the oxygen permeability higher compared to the other two mixes. In the cores taken in vertical direction the oxygen permeability of the covercrete at the top of the prisms always displays the highest values (Fig. 15). For the calculation of the coefficient of variation of the OP coefficient the covercrete was excluded.

The SCC displays identical values for oxygen permeability and water conductivity in vertical and horizontal direction. While the same applies for the oxygen permeability of CVC 1, its water conductivity is about 25% higher in horizontal direction. Both oxygen permeability and water conductivity of CVC 2 are slightly higher in vertical direction. The coefficient of variation of the OP coefficient is higher in horizontal direction in all mixes.

4. Discussion

4.1. Microscopy

Regarding the results there is a good agreement between the relative values for the volume of porous paste determined with the OM and the volume of pores determined with the ESEM respectively. The ratio of porous paste and pores between upper, lateral and lower ITZ in the different concrete mixes is similar.

The ESEM enables the analysis of individual pores with a much higher resolution than the OM, because the resolution with the latter is limited by the thickness of the thin sections. Furthermore, the volume of pores can be quantified in the

ESEM while the OM gives information about the relative porosity of a 30 μm thick slice of concrete by its relative luminescence. Another advantage of the ESEM versus the OM is the possibility to accurately identify cracks and define them as background. Some of the cracks present in the thin sections are not well defined due to the thickness of the samples and are therefore classified as "porous paste". The main advantage of the OM in comparison with the ESEM is its ease of operation and the fast data acquisition.

There is a certain latitude in defining the threshold for the different components which may affect reproducibility. In the ESEM images the difference in grey level values between pores and anhydrous cement to the paste is significant making the definition relatively easy. Due to the gradual transition between the different components in the thin sections the definition of a representative threshold is more challenging. On the other hand the volume of porous paste is not affected by this problem, because the illumination was kept constant for all samples. However, luminescence and with it the volume of porous paste may be affected by variations in the thickness of the thin sections.

4.2. Properties of the microstructure

The increased frequency of pores or porous patches in the ITZ cannot be explained only by poor particle packing due to the wall effect. In particular because there are significant differences between the upper, lateral and lower ITZ. The increased porosity below and at the side of the aggregates of the SCC compared to the top may be caused by accumulation of ascending pore fluids. Aggregates can function as a barrier to this ascending pore fluids leading to an increased porosity below and at the side of the aggregates. At the top of the aggregates there is no accumulation but rather a depletion of pore fluids resulting in the dense ITZ observed. Apart from the dosage of SP and the method of compaction the SCC and CVC 1 are identical including overall porosity. Therefore differences in the ITZ can be directly attributed to compaction. Regarding CVC 1 the accumulation of pore fluid must have been intensified due to the vibration induced by the vibrator during the casting of the concrete. Evidently this process leads to an increased porosity all around the aggregates as it is also seen for CVC 2. The higher porosity of the ITZ of CVC 1 compared to CVC 2 is possibly caused by the differences in water content and workability. Because of the differences in the rheological properties as indicated by the flow, CVC 1 may be more prone to an accumulation of pore fluid.

These results explain the contradiction about the anisotropy of the ITZ found in literature. While Hoshino [11] and Goldmann and Bentur [19] observed a wider ITZ below the aggregates than above, Crumbie [8] did not find a clear difference. Because the development of anisotropy is dependent on the compaction of the concrete and possibly on workability, the anisotropy may vary from concrete to concrete.

The increased oxygen permeability present in the covercrete of the vertical cores may be caused by several factors. The analysis of the images made with the OM shows no systematic difference in the porosity of the ITZ with depth while in the images made with the ESEM the porosity of the ITZ of the aggregates in the covercrete is slightly increased. Moreover, the relatively low bulk density of the covercrete suggests that the volume of aggregates is lower. Air voids were not covered in the analysis of the microstructure, but they might be the reason for the reduced bulk density. The higher oxygen permeability of the covercrete may also be attributed to the observed occurrence of microcracks perpendicular to the surface of the concrete caused by drying shrinkage.

4.3. Microstructure and permeability

The analysis of the images allows conclusions to be drawn about the distribution of the pores but not about their connectivity. Winslow et al. [5] used the hard core–soft shell model to calculate the influence of the thickness of the ITZ and the content of aggregates on the connectivity of pores in mortar and concrete. The model is based on the assumption that all aggregates are surrounded by a shell of homogeneous porosity. The model might be too simplified to explain connectivity and therefore be not realistic mainly due to the patchy distribution of the pores present in mortar and concrete [7,20].

According to the hard core–soft shell model the ITZ of a concrete with a volume of aggregates above 50% should be fully percolated [6]. The concrete mixes used in this study have a considerably higher volume of aggregates and the ITZ should therefore fully percolate. Consequently, their transport properties should be dependent on the width and porosity of the ITZ. The anisotropic distribution of pores in the ITZ could have an influence as well. Keller [12] measured water conductivity of bridge concrete and observed higher values in horizontal than in vertical direction. He supposed that the high porosity below aggregates observed by Hoshino [11] was responsible for this phenomenon. But in order to cause such a difference the combined permeability of the lower and upper ITZ has to be higher than the permeability of the lateral ITZ.

The differences in the concrete properties between the SCC and CVC 1 can be explained by the porosity of the ITZ. The ITZ of the SCC is narrower and less porous than that of CVC 1. Consequently, the SCC has higher strength, lower oxygen permeability and lower water conductivity than CVC 1. But the observed anisotropy in the ITZ of both concretes does not cause a systematic anisotropy in oxygen permeability or water conductivity; the oxygen permeability is identical in vertical and horizontal direction and the increased horizontal water conductivity observed with CVC 1 is not confirmed by the data obtained from the SCC. Obviously, there is no systematic difference in the combined permeability of the lower and upper ITZ compared to the lateral ITZ.

There seems to be some contradictions when only the porosity of the ITZ and its width are taken into consideration to explain the observed differences in the concrete properties between the SCC and CVC 2. Due to the slightly lower porosity in the ITZ, its anisotropy, the lower volume and smaller size of the aggregates, the SCC should show a lower permeability. This is not the case as the oxygen permeability is slightly higher and

the water permeability is clearly higher than in CVC 2. This indicates that other factors in addition to the ITZ contribute to the transport properties of the concrete mixes studied. Possibly the lower volume of paste of CVC 2 means that there is less penetrable volume and that the large aggregates are obstacles. The slightly increased oxygen permeability and water conductivity of CVC 2 in vertical direction could be the result of the slightly higher porosity in the lateral ITZ compared to the upper and the lower ITZ. In general, the reasons for differences in the properties of SCC and CVC of similar strength are difficult to assess due to frequent differences in volume of paste, type of cement and type of mineral admixtures. As a result, the conclusions from different studies can differ. For example, the oxygen permeability of SCC can be significantly lower than the one of CVC of similar strength [21], but it is also possible that both are in the same order of magnitude [22].

The microstructural observations clearly show that the pores in the ITZ and the bulk paste are distributed in a patchy manner. Because their frequency increases towards the interface the possibility of a connectivity of such patches increases. But the ITZ is not a shell of homogeneously increased porosity. The main problem in linking the porosity and the transport properties is the fact that little data about the real connectivity of pores exist. An attempt to directly identify connected pores by the intrusion of concrete with Wood's metal has shown that pores in the ITZ seem to be better connected than pores in the bulk paste [23]. But in order to really improve the data base the three dimensional connectivity of the pore system in cementitious materials would have to be studied.

5. Conclusions

The heterogeneity and microstructural complexity of the ITZ is a challenge for quantitative image analysis. For statistical reasons a large data base with hundreds of images is necessary to document compositional gradients on a profile through the interfacial zone. In addition, different localities at the top, at the sides and at the bottom of the aggregates have to be investigated systematically in order to characterize anisotropy caused by gravitational effects and the accumulation of pore fluid.

Optical microscopy on thin sections permits the distribution of porous paste in mortar and concrete to be to characterized, based on the definition of a "fluorescence threshold value". ESEM investigations on polished samples provide a higher resolution and enable discrete pores to be identified. For both methods constant imaging and segmentation parameters are crucial for the reproducibility of the results.

The software developed for quantitative image analysis enables characterization of continuous compositional profiles across the ITZ. It takes full advantage of the resolution of the images and enables an automated and reproducible quantification of the defined classes. In combination with the number of pictures analysed it provides a reliable data base for the comparison of ITZ porosity.

Compaction has a significant influence on the porosity and width of the ITZ. Therefore, the porosity of the ITZ of CVC is generally higher compared to SCC resulting in a lower compressive strength, higher oxygen permeability and higher water conductivity. However, the lower volume of paste and the generally larger aggregates used for CVC reduce these effects.

Considerable differences in the porosity of the lower, lateral and upper ITZ can occur. This fact is of great importance for investigations dealing with the microstructure of the ITZ. If it is not taken into account results may be of limited significance.

An anisotropic distribution of pores in the ITZ does not necessarily cause anisotropy in oxygen permeability and water conductivity.

In order to improve the understanding about the connectivity of pores in cementitious materials direct observations in three dimensions are necessary.

Acknowledgements

The authors would like to thank the staff of the concrete lab for producing the concrete and measuring its properties. L. Brunetti is acknowledged for the preparation of the samples used for microscopy.

References

[1] J. Farran, Contribution mineralogique à l'étude de l'adherence entre les constituants hydrates des ciments et les materiaux enrobes, Rev. Mater. Constr. 490/491 (1956) 191–209.
[2] K.L. Scrivener, A.K. Crumbie, P.L. Pratt, A study of the interfacial region between cement paste and aggregate in concrete, in: S. Mindess, S.P. Sha (Eds.), Bonding in Cementitious Composites, Materials Research Society, vol. 114, 1988, pp. 87–95.
[3] K.L. Scrivener, E.M. Gartner, Microstructural gradients in cement paste around aggregate particles, in: S. Mindess, S.P. Sha (Eds.), Bonding in Cementitious Composites, Materials Research Society, vol. 114, 1988, pp. 77–86.
[4] K.L Scrivener, P.L. Pratt, Characterisation of interfacial microstructure, in: J.C. Maso (Ed.), Interfacial Transition Zone in Concrete, RILEM Report, vol. 11, E. and F. N. Spoon, London, 1996, pp. 1–17.
[5] D.N. Winslow, M.D. Cohen, D.P. Bentz, K.A. Snyder, E.J. Garboczi, Percolation and pore structure in mortars and concrete, Cem. Concr. Res. 24 (1) (1994) 25–37.
[6] E.J. Garboczi, D.P. Bentz, Modelling of the microstructure and transport properties of concrete, Constr. Build. Mater. 10 (5) (1996) 293–300.
[7] S. Diamond, J. Huang, The interfacial transition zone: reality or myth? in: A. Katz, A. Bentur, M. Alexander, G. Arliguie (Eds.), The Interfacial Transition Zone in Cementitious Composites, E. and F.N. Spoon, London, 1998, pp. 1–37.
[8] A.K. Crumbie, PhD Thesis, University of London, 1994.
[9] K.L. Scrivener, A. Bentur, P.L. Pratt, Quantitative characterisation of the transition zone in high strength concrete, Adv. Cem. Res 1 (4) (1988) 230–237.
[10] J. Trägårdh, Microstructural features and related properties of self-compacting concrete, in: A. Skarendahl, Ö. Petersson (Eds.), Proceedings of the 1st International RILEM Symposium on Self-Compacting Concrete, Stockholm, 1999, pp. 175–186.
[11] M. Hoshino, Difference of the w/c ratio, porosity and microscopical aspect between the upper boundary paste and the lower boundary paste of the aggregate in concrete, Mat. Struct. 21 (125) (1988) 336–340.
[12] T. Keller, Dauerhaftigkeit von Stahlbetontragwerken: Transportmechanismen-Auswirkungen von Rissen, Doctoral Thesis ETH Zürich Nr. 9605, Zürich, 1992.
[13] A. Skarendahl, Ö. Petersson, Self-Compacting Concrete, RILEM Report, vol. 23, RILEM Publications, Cachan Cedex, 2000.

[14] O. Wallevik, I. Nielsson, Self-compacting concrete, Proceedings of the 3rd RILEM Symposium on Self-Compacting Concrete, Reykjavik, RILEM Publications S.A.R.L, Bagneux, 2003.
[15] T. Noguchi, H. Mori, State-of-the-art report: evaluation of fresh properties of self-compacting concrete in laboratory and on site, in: K. Ozawa, M. Ouchi (Eds.), Proceedings of the International Workshop on Self-Compacting Concrete, Kochi, 1998, pp. 97–110.
[16] EN 12350-5, Testing Fresh Concrete—Part 5: Flow Table Test, CEN European Committee for Standardization, Brussels, 2000.
[17] SN 562 162/1, Betonbauten: Materialprüfung, Schweizer Ingenieur-und Architektenverein, Zürich, 1995.
[18] M.G. Alexander, Y. Ballim, J.R. Mackechnie, Concrete durability index testing manual, Departments of Civil Engineering of University of Cape Town and University of the Witwatersrand, Research Monograph, vol. 4, 1999.
[19] A. Goldmann, A. Bentur, Effects of pozzolanic and non-reactive microfillers on the transition zone in high strength concrete, in: J.C. Maso (Ed.), Interfaces in Cementitious Composites, RILEM Proceedings, vol. 18, Chapman and Hall, London, 1993, pp. 53–61.
[20] S. Diamond, Percolation due to overlapping ITZs in laboratory mortars? A microstructural evaluation, Cem. Concr. Res. 33 (7) (2003) 949–955.
[21] W. Zhu, P.J.M. Bartos, Permeation properties of self-compacting concrete, Cem. Concr. Res. 33 (6) (2003) 921–926.
[22] A. Leemann, C. Hoffmann, Properties of self-compacting concrete — differences and similarities, Mag. Concr. Res. 57 (6) (2005) 315–319.
[23] K.L. Scrivener, K.L. Nemati, The percolation of pore space in the cement paste/aggregate interfacial zone of concrete, Cem. Concr. Res. 26 (1) (1996) 35–40.